Process Safety and Environmental Protection 173 (2023) 229–236

Contents lists available at ScienceDirect

Process Safety and Environmental Protection

journal homepage: www.journals.elsevier.com/process-safety-and-environmental-protection

Impact of oxygen and nitrogen-containing species on performance of NO removal by coal pyrolysis gas

Zhongze Bai [a], Xi Zhuo Jiang [b,*], Kai H. Luo [a,*]

[a] Department of Mechanical Engineering, University College London, Torrington Place, London WC1E 7JE, UK
[b] School of Mechanical Engineering and Automation, Northeastern University, Shenyang, Liaoning 110819, PR China

ARTICLE INFO

Keywords:
NO reduction
Oxygen and nitrogen-containing species
HCN
Reactive force field molecular dynamics

ABSTRACT

Coal pyrolysis gas is considered a promising reburn fuel with excellent NO reduction performance because of the present of nitrogen-containing species (HCN and NH_3) in the pyrolysis gas. In this study, we explored the effects of oxygen and nitrogen-containing species on NO removal performance with HCN and NH_3 by reactive force field (ReaxFF) molecular dynamics (MD) simulations. Results indicate that appropriately reducing O_2 concentrations and increasing the amount of nitrogen-containing species can benefit the NO reduction performance by coal pyrolysis gas. In addition, the effects of oxygen and nitrogen-containing species content on the NO removal and mechanisms of NO consumption and N_2 formation are illustrated during NO reduction with HCN and NH_3, respectively. Finally, based on the simulations results, practical operating strategies are proposed to optimize the NO reduction efficiency. In summary, this study provides new insights into NO reduction performance, which may contribute to optimizing the operating parameters to decrease NOx emissions during coal combustion.

1. Introduction

The nitrogen oxides (NOx) emissions from coal combustion cause serious environmental problems, such as photochemical smog and acid rain (Bowman, 1992). To mitigate its negative influence on environment during coal combustion, a few technologies have been invented recently. Those technologies can be divided into three categories: pre-combustion, combustion modification and post-combustion methods, where measures are implemented before, during and after the fuel combustion, respectively (Skalska et al., 2010). Among the many approaches, fuel reburning is a widely used, efficient and low-cost method to modify the fuel combustion process. It reduces NOx by transferring the generated NOx to harmless nitrogen (N_2) by reburn fuels, and thus the reburn fuels play an important role in NOx control. Many fuels have been used as reburn fuels such as coal, oil, natural gas, pyrolysis gas, etc. Coal pyrolysis (also termed as coal splitting and staging) achieves better performance than other reburn fuels during coal combustion, where NOx formed during coal combustion is reduced by pyrolysis gas form coal itself (Greul et al., 1996). The biggest challenge of this technology is the precise control of the operating parameters. To reduce NOx emissions efficiently, it is necessary to study the influence of operating conditions on NOx removal performance.

Greul and co-workers carried out experimental studies on the coal splitting and staging process (Greul et al., 1996). They pointed out that the optimum air/fuel ratio was around 0.9, and the nitrogenous species in the pyrolysis gas determined the NOx reduction behaviours. The same conclusion was also corroborated by Rüdiger and co-workers' work, where they found that the increase of nitrogenous species content of coal pyrolysis gas could improve the NOx removal performance (Rüdiger et al., 1997). Previous studies have demonstrated that the oxygen concentrations for reduction process and nitrogen-containing species content in pyrolysis are two important parameters for NOx removal. However, the underlying mechanisms of NOx reduction by nitrogen-containing species are still lacking. It is of great interest and importance to study the NOx reduction by nitrogen-containing species in coal pyrolysis gas under varying operating conditions, which may be helpful to control NOx emissions from coal combustion.

There are two types of nitrogen-containing compounds in coal pyrolysis gas, that is, hydrogen cyanide (HCN) and ammonia (NH_3) (Liu and Guo, 2017; Bai et al., 2022a). Besides, NO is considered as the main component of NOx emissions (accounting for up to 95%) (Glarborg et al., 2003; Wang et al., 2007). A variety of studies have been performed to investigate the NO reduction by NH_3 molecules in the selective non-catalytic reduction (SNCR) process, including its mechanisms and

* Corresponding authors.
E-mail addresses: jiangxz@mail.neu.edu.cn (X.Z. Jiang), k.luo@ucl.ac.uk (K.H. Luo).

https://doi.org/10.1016/j.psep.2023.03.007
Received 3 October 2022; Received in revised form 9 February 2023; Accepted 4 March 2023
Available online 7 March 2023

temperature influence on NO abatement abilities (Klippenstein et al., 2011; Cao et al., 2008). However, the above studies were carried out under fuel-lean conditions differing from the optimum air/fuel ratio of coal splitting and staging process, which could affect the NO removal performance with NH_3. In addition, the NO reduction process by HCN molecules has never been considered before. Recently, we investigated the underlying mechanisms during NO reduction by HCN and NH_3 molecules under varying temperatures by simulations (Bai et al., 2022b). We compared the performance of HCN and NH_3 in NO reduction process and the effects of temperature on their behaviours. We also investigated the influence of nitrogen-free species in coal pyrolysis gas on NO abatement behaviours (Bai et al., 2023a). However, a systematic comparison of the behaviours between the NO removal by HCN and NH_3 under varying O_2 and nitrogen-containing species content is still lacking.

To acquire a better understanding about the influence of the oxygen and nitrogen-containing species content on the performance of NO removal by HCN and NH_3, the investigation of reaction pathways is of great importance. However, it is extremely difficult or costly to obtain intermediates accurately because of the limitations of current experimental measurement methods. The reactive force field (ReaxFF) molecular dynamics (MD), an advanced computational method, has the potential to overcome this difficulty, which can simulate chemical processes with affordable computational costs (Jiang and Luo, 2021; Wang et al., 2023) and have been widely applied in the research of fuel pyrolysis and combustion (Wang et al., 2021; Bai et al., 2023b, 2023c).

In this study, ReaxFF MD simulations are performed to investigate the effects of oxygen and HCN or NH_3 content on NO reduction performance. The yields of NO and N_2 are studied firstly under varying oxygen and nitrogen-containing species concentrations. Then, the mechanisms of NO removal by HCN and NH_3 are explored, accounting for the NO reduction behaviours under different conditions. Finally, we establish the links between simulations and experimental results, and propose strategies regarding operating conditions to improve NOx reduction efficiency.

2. Methods

2.1. ReaxFF MD

ReaxFF employs a bond-order formalism in conjunction with polarisable charge descriptions to compute the reactive and non-reactive interactions between atoms. In ReaxFF, covalent and electrostatic interactions for a diverse range of materials are considered (Senftle et al., 2016). The potential energy can be calculated by (Ashraf and Van Duin, 2017):

$$E_{system} = E_{bond} + E_{over} + E_{under} + E_{lp} + E_{val} + E_{tor} + E_{vdWaals} + E_{Coulomb} \quad (1)$$

where E_{system}, E_{bond}, E_{over}, E_{under}, E_{lp}, E_{val}, E_{tor}, $E_{vdWaals}$, and $E_{Coulomb}$ represent total energy, bond energy, overcoordination energy penalty, undercoordination stability, lone pair energy, valence angle energy, torsion angle energy, van der Waals energy, and Coulomb energy, respectively (Ashraf and Van Duin, 2017).

2.2. Case set-ups

The equivalence ratios of reactants are calculated considering the reduction equation as follows:

$$4NO + 4HCN + 3\ O_2 \rightarrow 4\ N_2 + 2\ H_2O + 4CO_2 \quad (2)$$

$$4NO + 4NH_3 + O_2 \rightarrow 4\ N_2 + 6\ H_2O \quad (3)$$

To facilitate analysis, a molar ratio, λ, is proposed for HCN and NH_3 as shown in Eq. (4) and Eq. (5), respectively. R is the ratio of the number of HCN or NH_3 molecules to the number of pyridine molecules as shown in Eq. (6).

$$\lambda(HCN) = \frac{4n(O_2)}{3n(NO)} \quad (4)$$

$$\lambda(NH_3) = \frac{4n(O_2)}{n(NO)} \quad (5)$$

$$R = \frac{n(HCN\ or\ NH_3)}{n(NO)} \quad (6)$$

where n(NO), $n(O_2)$ and n(HCN or NH_3) represent the number of NO, O_2 and HCN or NH_3, respectively.

The mixtures simulated are summarized in Table 1. Cases 1 and 4 are for comparison under the λ and R values of 1 when NO is removed by HCN and NH_3, respectively. The data of cases 1 and 4 are from our previous work (Bai et al., 2022b). Cases 2 and 3 are set to investigate the effects of O_2 concentrations and HCN/NO ratios on NO abatement performance by HCN, where λ ranges from 0.0 to 0.8 and R ranges from 1.2 to 2.0 with an increment of 0.2. Similarly, Cases 5 and 6 are for the study of the number of O_2 and NH_3 molecules influence on NO reduction behaviours by NH_3 under varying λ and R values. By varying the size of the computational box, all the cases share the same density of 0.15 g/cm^3.

2.3. Simulation details

The canonical ensemble (NVT) (Andersen, 1980) is selected for ReaxFF MD simulations with a damping constant of 100 fs. At the beginning, every system undergoes energy minimization and equilibration for 20 ps at 40 K to optimize the initial geometric configuration. After that, the systems are heated to 3000 K and then the temperature is kept constant. The time step is 0.1 fs and total simulation time is 1000 ps for all simulations.

All the simulations are performed with the REAXC package in the LAMMPS software (Large-scale Atomic/Molecular Massively Parallel Simulator) (Aktulga et al., 2012; Plimpton, 1995) with C/H/O/N force field parameters (Zhang et al., 2009a, 2009b). Three replicas are carried out for every case with different initial configurations. The reaction pathways are analysed using Chemical Trajectory Analyzer (ChemTrayzer) scripts with the bond order cutoff of 0.3 (Döntgen et al., 2015). The net flux (NF) indicates how often the reaction was observed during the simulation time, which is calculated by the occurrence difference between the forward reaction and the reverse reaction (Arvelos and Hori, 2020).

3. Results

3.1. Effects of λ values on NO removal performance by HCN and NH_3

Fig. 1a and b show the numbers of NO and N_2 molecules during NO reduction by HCN and NH_3 under varying λ values at the end of the reactions, respectively. The number of NO increases with the O_2 concentrations, and the upward trend is more significant when NO is removed by HCN than NH_3. The N_2 formation is inhibited by high O_2 concentrations during NO reduction by NH_3. However, the N_2 generation shows a parabolic trend peaking at $\lambda = 0.6$ during NO reduction by HCN. This phenomenon is consistent with experimental studies that the

Table 1
Case set ups.

ID	Number of reactants	λ	R
1	120NO/120HCN/90 O_2	1.0	1.0
2	120NO/120HCN/0–72 O_2	0.0–0.8	1.0
3	120NO/144–240HCN/90 O_2	1.0	1.2–2.0
4	120NO/120NH_3/90 O_2	1.0	1.0
5	120NO/120NH_3/0–72 O_2	0.0–0.8	1.0
6	120NO/144–240NH_3/90 O_2	1.0	1.2–2.0

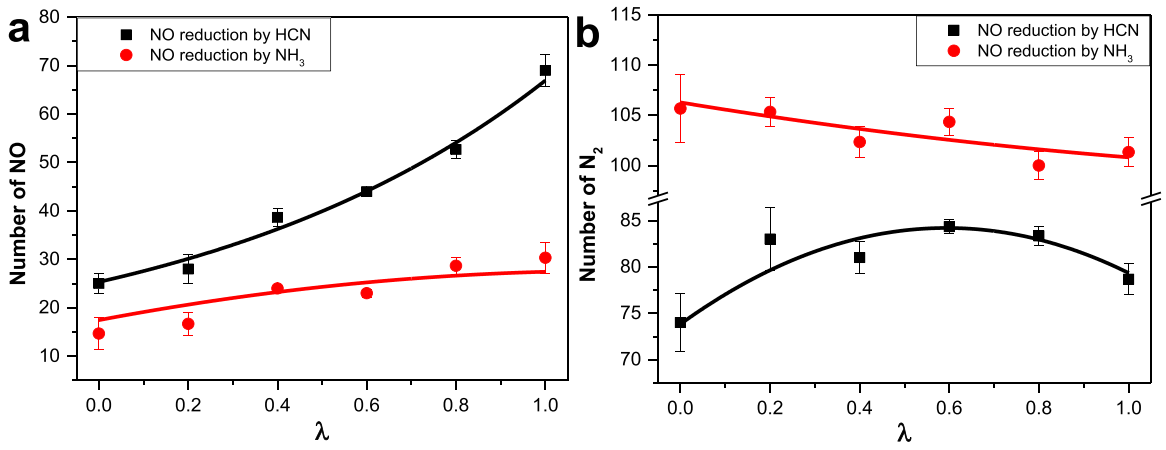

Fig. 1. Numbers of (a) NO and (b) N_2 for λ ranging from 0 to 1 at the end of simulations.

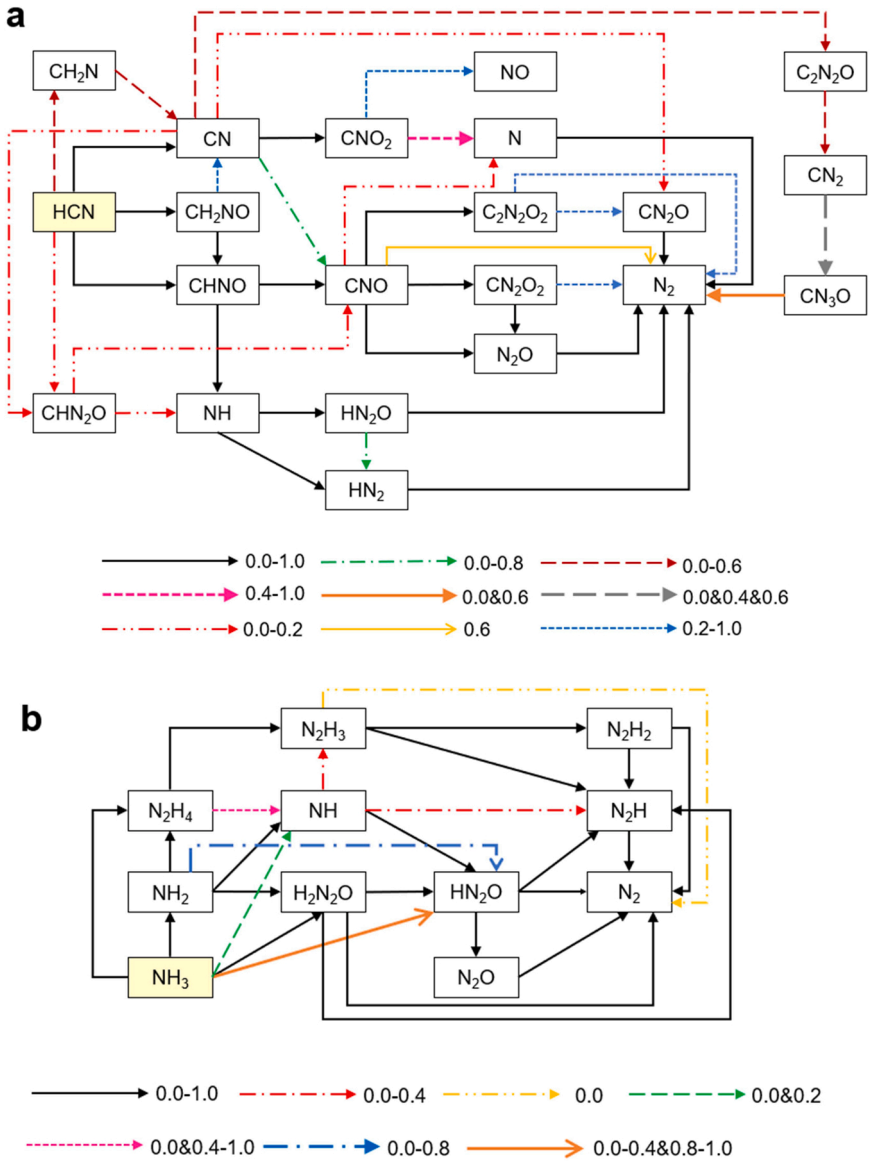

Fig. 2. Reaction pathways of NO reduction by (a) HCN and (b) NH_3 under varying λ values. HCN and NH_3 in the yellow box are the starting molecules.

optimum NOx reduction efficiency by coal pyrolysis gas is reached under fuel rich conditions (Greul et al., 1996).

To acquire a better understanding of how O_2 affects NO reduction by HCN and NH_3, reaction pathways at varying λ values are scrutinized in Fig. 2. According to Fig. 2a, CNO, NH and N are important intermediates for NO consumption in all cases. The reactions of NO consumption by HCN and CN are observed in $\lambda = 0.0$–0.2 cases. The generation of NO and N from intermediate CNO_2 is observed when λ is in the range of 0.2–1.0 and 0.4–1.0, respectively. CN_2 can react with NO forming CN_3O at $\lambda = 0.0$, 0.4 and 0.6. As to N_2 molecules, the thermal decomposition of intermediates HN_2O, HN_2, N_2O and CN_2O is found in $\lambda = 0.0$–1.0 cases. The reactions of CNO and N with NO generation occur in $\lambda = 0.6$ and 0.0–1.0 cases, respectively. The conversion from CN_3O to N_2 is observed in cases with λ at 0.0 and 0.6. The thermal decomposition of $C_2N_2O_2$ and CN_2O_2 is found when λ ranges from 0.2 to 1.0.

Fig. 2b illustrates reaction pathways during NO removal by NH_3. It is clear that the main intermediates remain the same in all cases, but the reaction pathways are different at varying O_2 concentrations during NO reduction process. Specifically, NH_3, NH_2 and NH are main intermediates to consume NO molecules and HN_2O, N_2H as well as N_2H_2 are key precursors for N_2 formation when λ values are 0.0–1.0. The pathway $N_2H_3 \rightarrow N_2$ is observed in the $\lambda = 0.0$ case. The pathways from NH_3 to HN_2O and N_2H_2 to NH are not found with λ at 0.6 and 0.2, respectively. The pathways $NH \rightarrow N_2H_3$, $NH \rightarrow N_2H$ and $H_2N_2O \rightarrow N_2H$ occur when λ values are within 0.0–0.4. The conversion from NH_3 to NH is observed with λ at 0.0 and 0.2.

To further identify how O_2 affects the numbers of NO and N_2 at the end of reactions, the NFs of main elementary reactions linked with N_2 and NO during NO reduction with HCN and NH_3 are investigated in Tables 2 and 3, respectively. As observed in Table 2, the NF of NO consumption fluctuates around 95 with λ rising from 0.0 to 1.0. But the NO formation through pathway $CNO_2 \rightarrow NO$ is enhanced at high O_2 concentrates during NO reduction by HCN leading to the net NO consumption decrease with λ increasing, which is consistent with the variation of NO numbers at different λ values in Fig. 2a. Although the influence of O_2 on the NF of NO consumption, the NFs of pathways linked with NO consumption are different at varying λ values. Specifically, the decrease in O_2 concentrations inhibits the pathways $CNO \rightarrow CN_2O_2$ and $CNO \rightarrow N_2O$ to consume NO, but enhances NO consumption by intermediates HCN, CN and CN_2. The NF of conversion from NH to HN_2O reaches the peak point at $\lambda = 0.4$. The effects of O_2 on $N \rightarrow N_2$ and $NH \rightarrow HN_2O$ are not significant.

Table 2
Net flux (NF) of main elementary pathways linked with NO and N_2 during NO removal with HCN at $\lambda = 0$–1.

Pathways	0	0.2	0.4	0.6	0.8	1
$HCN \rightarrow CHN_2O$	13	2	0	0	0	0
$CN \rightarrow CHN_2O$	11	7	0	0	0	0
$CN \rightarrow CN_2O$	15	6	0	0	0	0
$CNO \rightarrow N_2$	0	0	0	11	0	0
$CN_2 \rightarrow CN_3O$	7	0	10	10	0	0
$CNO \rightarrow CN_2O_2$	20	22	38	30	48	46
$CNO \rightarrow N_2O$	4	9	15	14	13	18
$N \rightarrow N_2$	5	7	6	6	8	6
$NH \rightarrow HN_2O$	13	20	23	22	22	17
$NH \rightarrow HN_2$	7	7	8	9	5	11
Total NO consumption	95	80	100	102	96	98
$CNO_2 \rightarrow NO$	0	8	14	31	45	60
Net NO consumption	95	72	86	71	51	38
$CNO \rightarrow N_2$	0	0	0	11	0	0
$CN_3O \rightarrow N_2$	10	0	0	7	0	0
$N_2O \rightarrow N_2$	20	48	45	42	45	54
$HN_2O \rightarrow N_2$	18	15	24	26	20	19
$CN_2O \rightarrow N_2$	8	11	11	17	16	19
$C_2N_2O_2 \rightarrow N_2$	0	8	7	13	14	19
$CN_2O_2 \rightarrow N_2$	0	11	5	12	13	17
$N \rightarrow N_2$	5	7	6	6	8	6
$N_2H \rightarrow N_2$	24	32	16	23	17	8
N_2 generation	85	132	114	157	133	142

Table 3
Net flux (NF) of main elementary pathways linked with NO and N_2 during NO removal with NH_3 at $\lambda = 0$–1.

Pathways	0	0.2	0.4	0.6	0.8	1
$NH \rightarrow HN_2O$	33	21	21	32	38	34
$NH \rightarrow N_2H$	7	7	14	0	0	0
$NH_2 \rightarrow H_2N_2O$	89	69	61	44	54	60
$NH_2 \rightarrow HN_2O$	4	12	8	22	14	0
$NH_3 \rightarrow HN_2O$	11	13	10	0	7	7
$NH_3 \rightarrow H_2N_2O$	22	29	22	20	23	18
Total NO consumption	166	151	136	118	136	119
$HN_2O \rightarrow N_2$	53	58	52	49	54	53
$N_2H \rightarrow N_2$	66	76	64	61	69	58
$N_2H_2 \rightarrow N_2$	30	34	28	17	23	18
$N_2O \rightarrow N_2$	23	18	21	19	26	15
$H_2N_2O \rightarrow N_2$	13	5	7	12	2	18
$N_2H_3 \rightarrow N_2$	11	0	0	0	0	0
Total N_2 formation	196	191	172	158	174	162

Regarding N_2 formation, the NF of N_2 formation shows a similar trend with the number of N_2 that peaks at $\lambda = 0.6$. Among the pathways of N_2 formation, O_2 benefits the pathways $CN_2O \rightarrow N_2$, $C_2N_2O_2 \rightarrow N_2$ and $CN_2O_2 \rightarrow N_2$ with λ ranging from 0.0 to 1.0. The contribution of $N_2O \rightarrow N_2$ almost remains the same with λ of 0.2–1.0, but it is significantly inhibited at $\lambda = 0.0$. O_2 molecules have insignificant influence on the conversion from N_2H to N_2 over $\lambda = 0.0$–0.6, but suppress this pathway in $\lambda = 0.8$–1.0 cases. The NF of pathway $N \rightarrow N_2$ changes slightly with λ increasing. The NF of N_2 formation from HN_2O reaches the highest point at $\lambda = 0.6$. Also, the pathways $CNO \rightarrow N_2$, $CN_3O \rightarrow N_2$ are found in $\lambda = 0.6$ and 0.0 & 0.6 cases, respectively.

According to Table 3, the NFs of NO consumption and N_2 formation show a decreasing trend with λ increasing, which agrees well with the variation of NO and N_2 numbers as shown in Fig. 1. Overall, the NF of NO reduction by NH radical almost remains the same with λ ranging from 0.0 to 1.0. When λ is lower than 0.4, the pathway $NH \rightarrow HN_2O$ is inhibited owing to the conversion from NH to N_2H. The contribution of NH_2 to NO reduction decreases significantly with the increase of O_2 concentrations. The contribution of $NH_2 \rightarrow H_2N_2O$, opposite to $NH_2 \rightarrow HN_2O$, shows parabolic trend reaching the lowest point in $\lambda = 0.6$. In addition, the reactions between NO and NH_3 molecules are inhibited slightly as the number of O_2 increases. As to N_2 generation, O_2 has little influence on pathways $HN_2O \rightarrow N_2$, $N_2O \rightarrow N_2$ and $H_2N_2O \rightarrow N_2$. At high λ values, the decrease of N_2 generation is through the inhibition of pathways $N_2H \rightarrow N_2$ and $N_2H_2 \rightarrow N_2$. Also, the conversion from N_2H_3 to N_2 is found in $\lambda = 0.0$.

To sum up, in the NO reduction with HCN cases, O_2 shows negative influence on the NO removal owing to the promotion of HCN oxidation forming NO molecules via the pathway $HCN \rightarrow CN \rightarrow CNO_2 \rightarrow NO$. Although the NF of NO molecules consumption almost remains the same under varying O_2 concentrations, the intermediates of NO consumption change from CN, HCN and CN_2 to CNO with λ increasing. O_2 molecules promotes the generation of CNO radical significantly, which can react with NO or itself (CNO) and generate N_2 eventually. However, the number of N_2 reaches maximum when λ is 0.6 due to the inhibition on the N_2 formation from HN_2O, N_2H, CN_3O and CNO when λ is greater than 0.6. Besides, the performance of NO removal and N_2 formation is supressed by O_2 under NO reduction by NH_3. That is because the NO consumption by NH_3 and NH_2 generating H_2N_2O or HN_2O is weakened as O_2 concentrations increase, which will be converted into N_2 eventually. Moreover, the increase of O_2 decreases the N_2 formation through the weakness of pathway $NH_3/NH_2/NH \rightarrow H_3N_2 \rightarrow H_2N_2 \rightarrow N_2$.

3.2. Effects of R values on NO removal performance by HCN and NH_3

As indicated in Fig. 3, the NO reduction and N_2 formation performance is enhanced by increasing *R* values in both NO reduction by HCN

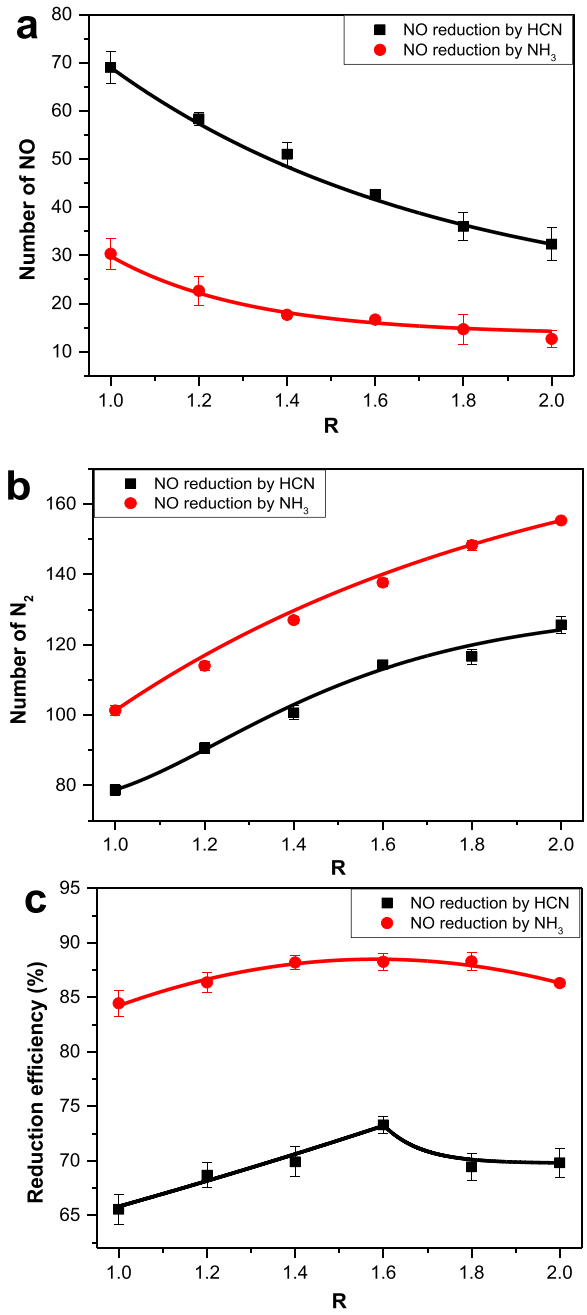

Fig. 3. The final number of (a) NO, (b) N_2 and (c) reduction efficiency at R = 1.0–2.0. Here, reduction efficiency is the ratio of nitrogen element in N_2 to nitrogen-containing reactants at the end of reactions.

and NH_3 cases. The reduction efficiencies of nitrogen-containing reactants rise by 7.7% and 3.8% with R increasing from 1.0 to 2.0, respectively. However, when R is larger than 1.6, their profiles present downward trends, which agrees well with previous work (Locci et al., 2018).

Fig. 4a illustrates reaction pathways of NO removal by HCN under varying R values. It is clear that high R values promote new intermediates and pathways to N_2 formation. Specifically, when R is larger than 1.2, the pathways CN → C_2N_2O → CN_2 → CN_3O → N_2, CN → CNO, CNO → N and HN_2O → N_2H are observed. The conversion from NH to N_2 and HN_2O to N_2O occur in R = 1.6–2.0 cases. The pathways generating N_2, CN → CHN_2O → N_2 and CN_2 → C_2N_3O → N_2, are found with R of 1.8 and 2.0. The conversion from N to N_2 is not observed in the R = 1.6 case. N_2 formation from CNO occurs when R values are 1.2, 1.6 and 1.8.

As shown in Fig. 4b, the main intermediates remain the same with the increase of R values during NO removal by NH_3 molecules. However, reactions pathways are different under varying R values. For instance, the pathways NH_2 → HN_2O and N_2H_3 → N_2 are found when R is larger than 1.2 and 1.8, respectively. The conversion from N_2H_4 to NH occurs in R = 1.0–1.8. The NH formation from NH_3 and conversion from NH to N_2H_3, N_2H_2 as well as N_2H are found in R = 1.6–2.0. The formation of N_2 from H_2N_2O is not observed with R of 1.2.

Fig. 4 shows the modification of reaction pathways during NO removal by HCN and NH_3 under different R values, but the reason why NO removal performance is enhanced by high R values is still unclear. To resolve this issue, the net flux (NF) of main elementary pathways linked with NO and N_2 during NO removal with HCN and NH_3 in R = 1.0–2.0 is scrutinized.

According to Table 4, the NF of NO abatement increases significantly, but the NO generation from CNO_2 decreases slightly with R rising, which accounts for the phenomenon that high R values enhance NO removal performance by HCN. The R values have little influence on the NF of N → N_2. The contribution of CNO on NO reduction reaches the peak value in the R = 1.4 case due to the pathways CNO → CN_2O_2 and CNO → N_2O. The pathways of NO consumption by CN, CN_2 and NH are promoted as R increases. More specifically, the NF of NH → HN_2O presents an upward trend in R = 1.0–1.6, however, decreases when R is larger than 1.6. The pathways NH → N_2H and NH → N_2 are enhanced with R of 2.0 and 1.6–2.0, respectively. Regarding N_2 generation, high HCN/NO ratios promote the generation of N_2 from CHN_2O, C_2N_3O, CN_3O, N_2H and NH. The NFs of CNO → N_2, N_2O → N_2 and N → N_2 fluctuate as R ranges from 1.0 to 2.0. High HCN/NH_3 ratios slightly weaken the pathway CN_2O_2 → N_2. As R increases, the N_2 formation from the pathway CNO → $C_2N_2O_2$/CN_2O → N_2 is enhanced in R = 1.0–1.6, but inhibited with R = 1.6–2.0.

When it comes to NO abatement by NH_3, the NO consumption with NH_3 molecules is enhanced with R increasing mainly through the pathway NH_3 → H_2N_2O as observed in Table 5. The conversion from NH to HN_2O and HN_2 almost remains the same under varying R values. Besides, as NH_3/NO ratios increase, the contribution of NH_2 to NO abatement (mainly through NH_2 → H_2N_2O) reduces first and then increases when R is larger than 1.4. As for N_2 generation, high R values promote the conversion from N_2H_3, N_2H and N_2H_2 to N_2. NH_3/NO ratios present little influence on the conversion from HN_2O to N_2 with R of 1.0–1.8, but enhance this pathway in the R = 2.0 case. The contribution of N_2O to N_2 generation decreases slightly with R rising. In addition, the NF of H_2N_2O to N_2 decreases with R increasing from 1.0 to 1.2, but presents upward trend when R is larger than 1.2.

In summary, the increase of HCN/NO and NH_3/NO ratios can promote NO removal performance, but the reduction efficiency peaks at the R value of 1.6. Specifically, the enhancement of NO removal is mainly by the promotion of the reactions of NH radical and NO molecules, and forming N_2 eventually. In addition, high R values also promote N_2 formation by adding new pathways HCN → CN → CHN_2O → N_2 and HCN → CN → C_2N_2O → CN_2 → CN_3O → N_2. Moreover, the "self-consumption" of HCN for N_2 formation through HCN → CNO → $C_2N_2O_2$/CN_2O → N_2 and HCN → CN → C_2N_2O → CN_2 → C_2N_3O → N_2 is enhanced with the rising HCN/NO ratios. Regarding NO abatement with NH_3, the increase of NH_3 molecules improves the NO reduction performance mainly by promoting the reaction of NO molecules with NH_3 and NH_2 to generate H_2N_2O, which will convert to N_2 finally. Also, the "self-consumption" effect of NH_3 is promoted by high R values via the conversion from N_2H_3 and N_2H_2 to N_2, which is produced by the reactions between NH_3, NH_2 and NH.

4. Discussion

ReaxFF MD is regarded as a first-principle simulation approach. The results are accurate and dependable if the chosen force field is sufficiently validated and correct numerical procedures are followed. The

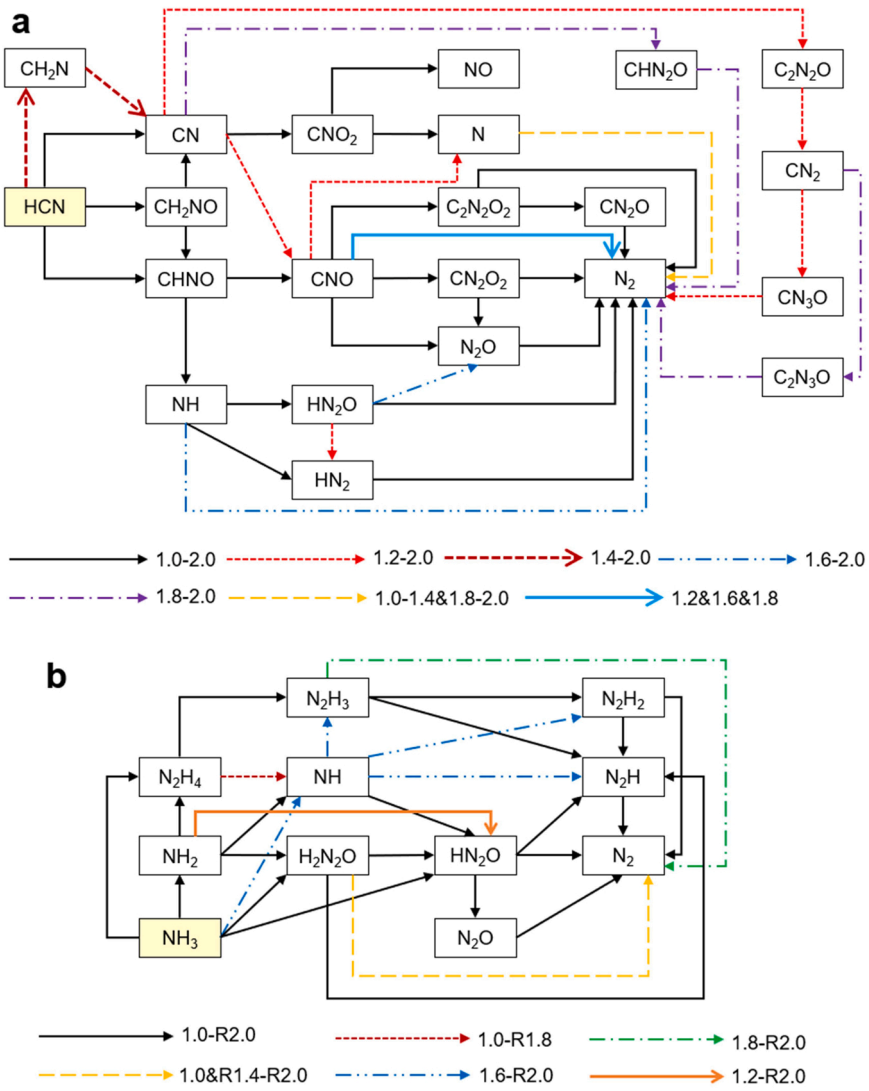

Fig. 4. Reaction pathways of NO reduction by (a) HCN and (b) NH_3 under varying R values. HCN and NH_3 in the yellow box are the starting molecules.

force field C/H/O/N used in the present study has been carefully validated against quantum chemistry calculations and experimental data available (Zhang et al., 2009a, 2009b). The results of the ReaxFF MD simulations thus provide uniquely detailed insights into the relevant chemical kinetics and pathways, which are hard if not impossible to obtain experimentally. On the other hand, simulating combustion at experimental temperatures using the ReaxFF MD method requires excessive computational costs and takes extremely long wall-clock time. It is a common practice for MD to adopt a higher temperature than those in experiments to ensure manageable computation time and cost. Fortunately, this approach has been verified to reproduce reaction mechanisms observed in experiments qualitatively well (Zhang et al., 2009a, 2009b), although there may be some quantitative differences.

In NO removal with HCN, O_2 molecules benefit the forming of important intermediates (CNO and NH), which can react with NO, and produce N_2 finally. However, O_2 also presents negative influence on NO abatement due to the NO formation by the oxidation of HCN, which accounts for the peak yields of N_2 in the $\lambda = 0.6$ case.

For the NO reduction by NH_3, O_2 only shows negative effects on its behaviours. Differing from the NO removal with HCN, species NH_3, NH_2 and NH can react with NO molecules generating N_2 without generating oxygen-containing intermediates firstly. However, O_2 molecules can combine with NH_i species forming macromolecules like $N_2H_6O_2$, $N_3H_9O_4$, $N_4H_{12}O_8$, $N_5H_{15}O_8$ and $N_6H_{18}O_8$. This process inhibits the reactions of NH_i and NO molecules, accounting for the negative influence of O_2 on NO reduction.

Considering there are both HCN and NH_3 in coal pyrolysis gas, the optimal λ is around 0.6 depending on the proportion of HCN and NH_3, which is smaller than the value (around 0.9) in previous experimental work (Greul et al., 1996). That may be caused by the inhibition of nitrogen-free species on the NO removal process under fuel-rich conditions. To obtain a better understanding of the influence of different nitrogen-free species (CH_4, CO and H_2) on NO removal, extended simulations with CH_4, CO and H_2 additives during the NO reduction with HCN and NH_3 are required.

In the NO removal process, the "self-consumption" phenomenon occurs in both HCN and NH_3 cases. That means the N_2 formation is from HCN and NH_3 itself without consuming NO molecules, causing the insufficient reducing agents. In addition, the oxidation of HCN forming NO is observed under the NO reduction with HCN cases, which also leads to the decrease of NO removal performance. Therefore, increasing the ratios of HCN and NH_3 over NO can increase the reduction efficiency, which reaches the highest point when R is 1.6 in both HCN and NH_3 cases. In real life, the ratios of nitrogen-containing species over NO can be controlled by the adjustment of operating parameters during coal pyrolysis such as temperature (Rüdiger et al., 1997), pressure (Liu and Guo, 2017) and water content (Bai et al., 2022a).

In coal pyrolysis gas, there are other substances like H_2S, COS, which

Table 4
Net flux (NF) of main elementary pathways linked with NO and N_2 during NO removal with HCN at $R = 1.0–2.0$.

Pathways	1.0	1.2	1.4	1.6	1.8	2.0
$CN \rightarrow CHN_2O$	0	0	0	0	3	6
$CN_2 \rightarrow CN_3O$	0	10	7	18	14	22
$CNO \rightarrow N_2$	0	14	0	6	5	0
$CNO \rightarrow CN_2O_2$	46	38	60	47	34	45
$CNO \rightarrow N_2O$	18	10	23	13	17	8
$N \rightarrow N_2$	6	10	10	0	8	8
$NH \rightarrow HN_2O$	17	24	40	43	31	35
$NH \rightarrow N_2H$	11	12	8	13	11	17
$NH \rightarrow N_2$	0	0	0	11	5	17
NO consumption	98	118	148	151	128	158
$CNO_2 \rightarrow NO$	60	54	55	49	45	45
Net NO consumption	38	64	93	102	83	113
$CHN_2O \rightarrow N_2$	0	0	0	0	13	8
$C_2N_3O \rightarrow N_2$	0	0	0	0	10	9
$CNO \rightarrow N_2$	0	14	0	6	5	0
$CN_3O \rightarrow N_2$	0	5	6	7	3	13
$N_2O \rightarrow N_2$	54	42	48	36	49	47
$HN_2O \rightarrow N_2$	19	26	32	41	29	36
$CN_2O \rightarrow N_2$	19	28	25	27	27	24
$C_2N_2O_2 \rightarrow N_2$	19	13	17	19	17	17
$CN_2O_2 \rightarrow N_2$	17	11	12	9	8	12
$N \rightarrow N_2$	6	10	10	0	8	8
$N_2H \rightarrow N_2$	8	19	21	28	31	37
$NH \rightarrow N_2$	0	0	0	11	5	17
N_2 generation	142	168	171	184	205	220

Table 5
Net flux (NF) of main elementary pathways linked with NO and N_2 during NO removal with NH_3 at $R = 1.0–2.0$.

Pathways	1.0	1.2	1.4	1.6	1.8	2.0
$NH_3 \rightarrow HN_2O$	7	10	11	10	4	12
$NH_3 \rightarrow H_2N_2O$	18	27	48	45	34	66
$NH_2 \rightarrow H_2N_2O$	60	44	40	64	75	78
$NH_2 \rightarrow HN_2O$	0	8	12	8	12	2
$NH \rightarrow HN_2O$	34	37	36	30	28	24
$NH \rightarrow HN_2$	0	0	0	4	10	10
NO consumption	119	126	147	161	163	192
$HN_2O \rightarrow N_2$	53	53	53	54	50	66
$N_2H \rightarrow N_2$	58	91	98	137	144	145
$N_2H_2 \rightarrow N_2$	18	29	34	55	58	65
$N_2O \rightarrow N_2$	15	23	13	11	20	6
$H_2N_2O \rightarrow N_2$	18	0	8	6	14	22
$N_2H_3 \rightarrow N_2$	0	0	0	0	14	15
N_2 generation	162	196	206	263	300	319

may affect the NO reduction process. Besides, developing suitable catalysts for NOx removal by coal pyrolysis gas is also a promising way for NOx control (Ye et al., 2020; Lu et al., 2021a, 2021b). Further investigations are needed to provide quantitative information.

5. Conclusions

In this study, ReaxFF simulations are performed to explore the mechanisms of NO reduction under varying O_2 and nitrogen-containing species (HCN and NH_3) content, respectively. Firstly, we obtained the numbers of NO and N_2 at the end of reactions in NO reduction by HCN and NH_3 under varying conditions. Results indicate that appropriately decreasing O_2 concentrations and increasing the number of nitrogen-containing species can improve the NO reduction performance by coal pyrolysis gas. Such phenomena are explained at the atomic level through the analysis of reaction pathways and NFs of each reaction. To sum up, this research provides new insights into the influence of oxygen and nitrogen-containing species content on NO reduction performance, which can potentially contribute to optimisation of operating conditions to achieve lower NOx emissions during coal combustion.

Declaration of Competing Interest

The authors declare that they have no known competing financial interests or personal relationships that could have appeared to influence the work reported in this paper.

Acknowledgement

Support from the UK Engineering and Physical Sciences Research Council under the project “UK Consortium on Mesoscale Engineering Sciences (UKCOMES)” (Grant Nos. EP/R029598/1 and EP/X035875/1) is gratefully acknowledged. This work made use of computational support by CoSeC, the Computational Science Centre for Research Communities, through UKCOMES.

References

Aktulga, H.M., Fogarty, J.C., Pandit, S.A., Grama, A.Y., 2012. Parallel reactive molecular dynamics: numerical methods and algorithmic techniques. Parallel Comput. 38 (4–5), 245-59.
Andersen, H.C., 1980. Molecular dynamics simulations at constant pressure and/or temperature. J. Chem. Phys. 72 (4), 2384-93.
Arvelos, S., Hori, C.E., 2020. ReaxFF study of ethanol oxidation in O_2/N_2 and O_2/CO_2 Environments at high temperatures. J. Chem. Inf. Model. 60 (2), 700-13.
Ashraf, C., Van Duin, A.C., 2017. Extension of the ReaxFF combustion force field toward syngas combustion and initial oxidation kinetics. The. J. Phys. Chem. A 121 (5). :1051-68.
Bai, Z., Jiang, X.Z., Luo, K.H., 2022a. Effects of water on pyridine pyrolysis: a reactive force field molecular dynamics study. Energy 238, 121798.
Bai, Z., Jiang, X.Z., Luo, K.H., 2022b. A reactive molecular dynamics study of NO removal by nitrogen-containing species in coal pyrolysis gas. Proc. Combust. Inst.
Bai, Z., Jiang, X.Z., Luo, K.H., 2023a. Effects of nitrogen-free species on NO removal performance by coal pyrolysis gas via reactive molecular dynamics simulations. J. Energy Inst., 101172
Bai, Z., Jiang, X.Z., Luo, K.H., 2023b. Reactive force field molecular dynamics simulation of pyridine combustion assisted by an electric field. Fuel 333, 126455.
Bai, Z., Jiang, X.Z., Luo, K.H., 2023c. Understanding mechanisms of pyridine oxidation with ozone addition via reactive force field molecular dynamics simulations. Chem. Eng. Sci. 266, 118290.
Bowman C.T. Control of combustion-generated nitrogen oxide emissions: technology driven by regulation. Symposium (International) on Combustion. 1992;24(1): 859–78.
Cao Q., Liu H., Wu S.-H., Zhao L.-P., Huang X. Kinetic study of promoted SNCR process by different gas additives. 2008 2nd International Conference on Bioinformatics and Biomedical Engineering. 2008:4034–8.
Döntgen, M., Przybylski-Freund, M.-D., Kröger, L.C., Kopp, W.A., Ismail, A.E., Leonhard, K., 2015. Automated discovery of reaction pathways, rate constants, and transition states using reactive molecular dynamics simulations. J. Chem. Theory Comput. 11 (6), 2517–2524.
Glarborg, P., Jensen, A., Johnsson, J.E., 2003. Fuel nitrogen conversion in solid fuel fired systems. Prog. Energy Combust. Sci. 29 (2), 89–113.
Greul U., Spliethoff H., Magel H.-C., Schnell U., Rüdiger H., Hein K., et al. Impact of temperature and fuel-nitrogen content on fuel-staged combustion with coal pyrolysis gas. Symposium (International) on Combustion. 1996;26(2):2231–9.
Jiang, X.Z., Luo, K.H., 2021. Reactive and electron force field molecular dynamics simulations of electric field assisted ethanol oxidation reactions. Proc. Combust. Inst. 38 (4), 6605-13.
Klippenstein, S.J., Harding, L.B., Glarborg, P., Miller, J.A., 2011. The role of NNH in NO formation and control. Combust. Flame 158 (4), 774-89.
Liu, J., Guo, X., 2017. ReaxFF molecular dynamics simulation of pyrolysis and combustion of pyridine. Fuel Process. Technol. 161, 107-15.
Locci, C., Vervisch, L., Farcy, B., Domingo, P., Perret, N., 2018. Selective non-catalytic reduction (SNCR) of nitrogen oxide emissions: a perspective from numerical modeling. Flow., Turbul. Combust. 100 (2), 301-40.
Lu, P., Ye, L., Yan, X., Fang, P., Chen, X., Chen, D., et al., 2021a. Impact of toluene poisoning on MnCe/HZSM-5 SCR catalyst. Chem. Eng. J. 414, 128838.
Lu, P., Ye, L., Yan, X., Chen, X., Fang, P., Chen, D., et al., 2021b. N2O inhibition by toluene over Mn-Fe spinel SCR catalyst. J. Hazard. Mater. 414, 125468.
Plimpton, S., 1995. Fast parallel algorithms for short-range molecular dynamics. J. Comput. Phys. 117 (1), 1–19.
Rüdiger, H., Greul, U., Spliethoff, H., Hein, K.R., 1997. Distribution of fuel nitrogen in pyrolysis products used for reburning. Fuel 76 (3), 201–205.
Senftle, T.P., Hong, S., Islam, M.M., Kylasa, S.B., Zheng, Y., Shin, Y.K., et al., 2016. The ReaxFF reactive force-field: development, applications and future directions. npj Computational. Materials 2 (1), 1–14.
Skalska, K., Miller, J.S., Ledakowicz, S., 2010. Trends in NOx abatement: a review. Sci. Total Environ. 408 (19), 3976–3989.
Wang, J., Jiang, X.Z., Luo, K.H., 2023. Exploring reaction mechanism for ammonia/methane combustion via reactive molecular dynamics simulations. Fuel 331, 125806.

Wang, Y., Li, Y., Zhang, C., Yang, L., Fan, X., Chu, L., 2021. A study on co-pyrolysis mechanisms of biomass and polyethylene via ReaxFF molecular dynamic simulation and density functional theory. Process Saf. Environ. Prot. 150, 22–35.
Wang, Z., Zhou, J., Zhu, Y., Wen, Z., Liu, J., Cen, K., 2007. Simultaneous removal of NOx, SO_2 and Hg in nitrogen flow in a narrow reactor by ozone injection: experimental results. Fuel Process. Technol. 88 (8), 817-23.
Ye, L., Lu, P., Chen, X., Fang, P., Peng, Y., Li, J., et al., 2020. The deactivation mechanism of toluene on MnOx-CeO2 SCR catalyst. Appl. Catal. B: Environ. 277, 119257.
Zhang, L., Duin, A.Cv, Zybin, S.V., Goddard Iii, W.A., 2009a. Thermal decomposition of hydrazines from reactive dynamics using the ReaxFF reactive force field. J. Phys. Chem. B 113 (31), 10770–10778.
Zhang, L., Zybin, S.V., Van Duin, A.C., Dasgupta, S., Goddard III, W.A., Kober, E.M., 2009b. Carbon cluster formation during thermal decomposition of octahydro-1, 3, 5, 7-tetranitro-1, 3, 5, 7-tetrazocine and 1, 3, 5-triamino-2, 4, 6-trinitrobenzene high explosives from ReaxFF reactive molecular dynamics simulations. The. J. Phys. Chem. A 113 (40), 10619–10640.